

Optimization for Solving Workcell Layouts using Gaussian Penalties for Escaping Local Minima

Thomas Fridolin Iversen and Lars-Peter Ellekilde

The Maersk McKinney Moller Institute, University of Southern Denmark, Campusvej 55, 5230, Odense M, Denmark

Keywords: Robot Workcell Optimization, Optimization Algorithms, Industrial Robotics.

Abstract: The main contribution of this paper is a method for optimizing the layout of workcells taking into consideration both the reachability of the robot as well as the expected cycle time. To analyse the reachability for systems using sensors to pose estimate objects, the method uses a combination of discrete samples over the space in which objects are located and a manipulability measure based on the determinant of the manipulator Jacobian. To compute the expected cycle time for the robot, the method includes a simulated controller, which is optimized to estimate the performance of the physical robot. For the optimization of the workcell layout the proposed method based on applying Gaussian penalties in local minima is compared to three existing methods for global optimization. For the optimization of the simulated controller three different local methods are compared along with one global.

1 INTRODUCTION

Utilizing robots in industrial tasks, such as bin-picking and product assembly, means having the robots work in environments, which includes a multitude of entities such as machines, fixtures, feeders, bins with randomly placed objects etc. Optimizing the layout of a workcell to ensure that all entities are reachable can be challenging and even more so when the location of objects are not known before hand, but identified online using a sensor system. Trying manually to adjust the workcell layout to reduce the cycle time can be even more challenging, as a longer but simpler trajectory might well be faster than one being shorter but more complex.

In this paper, a formulation of the workcell layout problem is suggested where the objective includes both reachability, but also an estimate of the actual execution times for the robot. To support scenarios where objects poses are estimated in a bin or on a feeder, the method will use a combination of discrete samples over the space of expected object poses and a manipulability measure based on the determinant of the manipulator Jacobian. To estimate the execution times for the robot, a simulation of the robot controller is needed. To that end, a model based on parabolic blends (Petersen and Ellekilde, 2011) is used, and parameters scaling the acceleration and velocity limits as well as blend values are optimized for

tuning the model to match the properties of the physical robot. The input to this optimization is a collection of representative trajectories executed on the real robot. Collecting these data can be time consuming, hence four different optimization algorithms has been compared to see how well they perform on a limited set of data.

The use of the manipulability metric helps smooth the objective compared to just using discrete samples, but it is impossible to guarantee that the objective will have no local minima. Also when combined with the estimates of execution times, we risk introducing local minima in the overall objective function. To cope with these, this paper proposes an optimization algorithm based on the complete Fill Algorithm (Morris, 1993), which seeks to escape local minima by adding a virtual force, pushing it away. Even though the proposed algorithm is not proven complete in the sense that it will always find the optimal solution, then we will argue that in the limit it will be equivalent to the Fill Algorithm. Furthermore when tested in practice it performs very well on the layout optimization problem.

To further improve the optimization, a starting point sampling method is suggested, using spherical sampling around the robot. Additionally is a comparison done, where three other global algorithms are tested against the suggested one, with and without starting point sampling. The tested algorithms are

chosen to represent the three main categories of global derivative free optimization methods being deterministic, model-based and stochastic.

The rest of this paper is organized with related work in Section 2, the overall objective function is introduced in Section 3, the description of the optimized simulation of the robot controller in Section 4, a description and discussion of the proposed method along with a presentation of the tests in Section 5, experimental results in Section 6 and a conclusion in Section 7.

2 RELATED WORK

This section is divided in two parts, the first being work related to the optimization of robotic workcells and the second part being general optimization techniques.

2.1 The Robotic Workcell Layout Problem

A problem closely related to the optimization of robotics workcells is the facility layout problem (FLP) (for a general introduction see (Arabani and Farahani, 2012)). FLP is generally concerned with placing a number of machines to minimize a cost function, typically transportation time of objects, and comes in many forms: Static and dynamic FLP variations are concerned with whether the cost function is changing over time; for lower dimensionality the Single-row facility layout problem is utilized and both discrete and continuous versions are described in literature.

An important difference between FLP and the presented workcell optimization is that for FLPs the vertical dimension of the environment is not considered, constraining the problem to 2D position and a single rotation around the vertical axis. Furthermore the robot kinematics and dynamics are ignored, hence the cost function only depends on distances and flows between machines, see e.g. (Zhang and Li, 2009), (Gonçalves and Resende, 2015) or (Guan and Lin, 2016) for applications of FLP.

A 3D case of workcell optimization is found in (Cagan et al., 1998), where components are decomposed into containers and the objective is to maximize the packing density. (Gueta et al., 2009) also optimizes workcell layouts in 3D, but the objective function only consists of a simple time measure and spatial requirements, thus the reachability and robot execution times are not considered.

In (Lim et al., 2016) the authors utilize 5 different nature inspired algorithms to optimize a workcell layout for assembly tasks. Although only considering the discrete 2D case, robot kinematics are considered via the manipulability of the robot along with execution time and layout area. These include the same objectives as used in this paper, but calculated and weighted differently. The layout area is weighted the most, followed by the execution time and lastly the manipulability. As our manipulability measure also covers how many objects the robot can reach, it is weighted the highest and the execution time is then prioritized second. Furthermore our approach depends on a more elaborated simulation of the execution times, including path planning and a simulation of execution times optimized to approximate the physical robot. Minimizing the layout area, even though considered an important property for transporting objects in a facility (Koopmans and Beckmann, 1957), is for now not a part of our objective function and we rely on boundary constraints to prevent components from moving outside the space of the workcell.

2.2 Optimization Algorithms

A common property of the optimization objectives considered in this paper is, that they are not analytically differentiable, hence we will have to rely on methods for derivative-free optimization, for which a general review can be found in (Rios and Sahinidis, 2013), together with an evaluation of different software packages. Details of the chosen algorithms are given in Sections 4.1 and 5.4 in connection with the objective functions and the results.

A specific problem in optimization is overcoming local minima, for which research have been carried out within different domains. In motion planning, (Barraquand and Latombe, 1991) uses Brownian motions to escape local minima, while (Barraquand et al., 1992) maps local minima in the workspace with a potential field planner and connects those in a graph structure which can be searched for a path. The work in (Park and Lee, 2003) places virtual obstacles in an environment to avoid getting stuck in local minima, when applying a potential field planner. In (Morris, 1993) two methods are presented, the first being the Breakout algorithm applying forces to the different parameters trying to force it out of a local minima and secondly the more abstract Fill Algorithm, which is proven to be complete for discrete problems. The proposed method in the paper is very similar to the Breakout and Fill Algorithms, but is concretized with a Gaussian penalty for filling.

Simulated annealing, first proposed for combina-

torial problems by (Kirkpatrick et al., 1983) and later generalized for continuous problems by (Bélisle et al., 1993), is a probabilistic algorithm that tries to overcome local minima by taking steps, that does not necessarily optimize the objective function, based on a decreasing probability reminiscent of that of a annealing mechanical system. The method shares properties with the also probabilistic Evolutionary Algorithm (Holland, 1975) which is used for testing in section 6.

3 OPTIMIZATION OBJECTIVE

The main goal of the optimization is to find a layout of the workcell that maximizes the reachability, referred to as $r(x)$ of the robot while minimizing the execution times, referred to as $t(x)$. Details of how the reachability and execution times are defined can be found below in Sections 3.1 and 3.2. Alternative criteria such as e.g. safety (average clearance between robot and obstacles) or energy consumption could also be considered as objectives, but would require the definition of appropriate objective functions that can either replace or supplement the reachability and execution time.

Having a dual purpose a scaling is required to weigh the objectives, hence the overall objective function becomes

$$\underset{x \in X}{\text{minimize}} \quad f(x) = w_t \cdot t(x) + w_r \cdot r(x) \quad (1)$$

where w_r and w_t are the scaling of reachability and execution times, respectively. X is the space of all feasible parameter values, meaning those where the entities are not colliding and all fixed and required targets are reachable. x is a concrete set of parameters corresponding to a specific pose of all entities in the workcell. Here it is important to choose the parameter set to be minimal, as the optimization problem may otherwise not have a well defined minimum.

While the theoretical definition of X is rather straight forward, it is hard to define practically. To effectively restrict the solutions to X the objective function will return large values for infeasible states. To still guide the optimization towards feasible areas this value will depend on how many of the required targets that are indeed reachable.

3.1 Reachability

When considering applications that include picking randomly placed objects from feeders and bins, it is important that the reachability measure reflects the ability to pick as many objects as possible. In these

cases targets are distributed across a bounded subspace of $SE(3)$, meaning that we can approximate the distribution with a finite set of samples, S . Just counting the number of samples that are reachable would result in the objective becoming a step function and would require a very large number of samples to represent the reachability well. To get a more smooth function the manipulability proposed in (Yoshikawa, 1985) is used to indirectly score reachable samples depending on how likely it is, that nearby objects would also be reachable. This measure is computed as $\sqrt{\det(J(q)J(q)^T)}$, where $J(q)$ is the manipulator Jacobian and q is the joint configuration for reaching the target. For unreachable points without an inverse kinematics solution a manipulability measure of 0 is used. The manipulability score for a parameter set x and sample s can thus be described as:

$$m(x, s) = \begin{cases} \sqrt{\det(J(q)J(q)^T)}, & \text{if IK}(x, s) \neq 0. \\ 0, & \text{otherwise.} \end{cases} \quad (2)$$

where $q = IK(x, s)$ is the inverse kinematics solution for sample s and the parameter set x . If no inverse kinematics solution exists $IK(x, s)$ will return 0.

To penalize configurations with close-to zero manipulability, the measure can be raised to a constant $0 < p < 1$, where we empirically found that $p = \frac{1}{4}$ gives good results for our scenarios. The complete reachability score is then computed over all samples as

$$r(x) = \frac{1}{N} \sum_i^{N-1} m(x, s)^p \quad (3)$$

where N is the number of samples in S .

3.2 Execution Times

When working in industrial environments, time spent moving a robotic arm is generally a limiting factor when considering cycle times and productivity. It is therefore considered in the objective function by

$$t(x) = \frac{1}{M} \sum_{i=0}^{N-1} t_i(x) \quad (4)$$

where M is the number of cycles, equal to the number of reachable samples, and $t_i(x)$ is the time taken for the cycle associated with the i th sample and estimated using the simulation optimized to mimic the physical robot, as described in Section 4.

To actually define the robot motions in a cycle a motion planner is used to determine the trajectories.

A challenge with classic planning techniques, such as the Rapidly-Exploring Random Tree (LaValle, 1998), is that they are probabilistic, meaning that the objective score may change between two evaluations. To overcome this problem the deterministic TrajOpt algorithm is chosen, see (Schulman et al., 2014), as it has shown promising results to similar cases in (Iversen and Ellekilde, 2017). To remove further noise in the objective function, the upper and lower 10% of execution times are removed when calculating the mean execution time of all cycles to get rid of outliers.

4 OPTIMIZATION OF EXECUTION TIMES SIMULATION

To minimize execution times in the workcell optimization it is necessary to efficiently estimate the duration of robot motions. Some manufacturers offer offline simulations of their robot controllers, e.g. (Universal Robots, 2017), (ABB Robotics, 2017) and (FANUC, 2017), but these work in real time and are not easily integrated into an optimization problem. To have a more computationally efficient estimate of execution times and avoid a full dynamic simulation of the robot, the model of (Petersen and Ellekilde, 2011) based on parabolic blends and velocity and acceleration limits is used.

Real world execution times might be influenced by other things beside acceleration and velocity limits, hence the model is not completely accurate. However, to enhance predictions an optimization of the method is implemented, where the parameters to be optimized are velocity and acceleration scalings along with a scaling of the blends distances. The acceleration and velocity scalings are multiplied with the given accelerations and velocities limits when running the model, while the blend scaling is used to alter the maximum allowed deviation when blending through configurations. While some robots, such as the Universal Robots, blends in Cartesian coordinates while (Petersen and Ellekilde, 2011) utilizes blends in configuration space, the blend scaling parameter helps adapt between the two. Blending in different spaces means that paths joint configuration will differ from each other, however only the time taken to move the robot is needed and the path differences can be ignored.

The objective function to optimize for tuning the

simulation thus becomes

$$\underset{\alpha, \beta, \gamma}{\text{minimize}} \frac{1}{N} \sum_{i=0}^{N-1} \|t_i^b(\alpha, \beta, \gamma) - t_i^e\| \quad (5)$$

where N is the number of executed paths, t_i^b and t_i^e are respectively the time estimated by the parabolic blend method and the actual execution time on the robot for the i 'th path. α , β and γ are the velocity, acceleration and blend scalings, respectively.

Collecting the paths for optimizing the simulation parameters can be time consuming, hence it is desirable to compare how different optimization methods performs on the same set of data. Section 4.1 presents these results for four different optimization algorithms.

4.1 Test of Execution Times Simulation

250 paths are executed on a real-life Universal Robots UR5 robot to obtain data, of which 80% are used for training and 20% for verification. The paths should be representative for the problem, hence they are extracted from running the application with an unoptimized workcell.

Assuming that the optimization problem is rather well-behaved, four optimization algorithms are used to optimize the parameters. The first two are the conjugate gradient descent (CGD) and Broyden-Fletcher-Goldfarb-Shanno (BFGS) algorithms both from the dlib library (King, 2009). These are purely local and tested to determine the impact of using a numerical estimate of the gradient.

Also from (King, 2009) BOBYQA (Powell, 2009) is tested as it have shown good performance in (Rios and Sahinidis, 2013). BOBYQA relies on an interpolation forming quadratic models of a trust region and is derivative free. Still being rather local, it uses a more complex analysis of the neighborhood compared to that of CGD and BFGS.

To test a global algorithm, RBFopt (Costa and Nannicini, 2014) is chosen to see whether a global approach will converge to the same result as the local ones. RBFopt uses Radial Basis functions to approximate the objective function and uses multiple approximations with cross validation to select the best fit. Updating the approximation is done with balancing exploration and exploitation on a global scale, making it a global solver in contrast to the other three.

The algorithms are tested with 500 different seed points and their end results are verified. Using different random seed points for CGD and BFGS is straight forward, but it is somewhat more complex for BOBYQA and RBFopt. Since BOBYQA requires a trust region around seeds it is necessary to limit

the sampling space. Thus, when using a thrust region of 1/10 of the range of the parameters, the seed points for BOBYQA can only be placed in mid 8/10 of the range. To gain a fair comparison, seed points for CGD and BFGS are therefore also only placed in this space. RBFopt relies on multiple seed points to form the initial function approximation. To generate these seed points RBFopt uses Latin Hypercube sampling. Given the different seed sampling methods, it is hard to do a completely fair comparison, but the differences should be close to negligible.

Results from the test can be seen in Figure 1 and Table 1, where scores obtained on training data and on verification data are presented along with number of objective function evaluations. BOBYQA manages to find the best set of parameters, both for the evaluated objective function and for the verification. It does so at a cost though, as it requires more than twice as many function evaluations as RBFopt, for finding a slightly better solution. In general all solutions varies under 0.2 seconds in mean time from the executed path times on the real robot, which given the length of the executed paths of 6-8 seconds are a maximum error of 3% and down to 1.25% for BOBYQA.

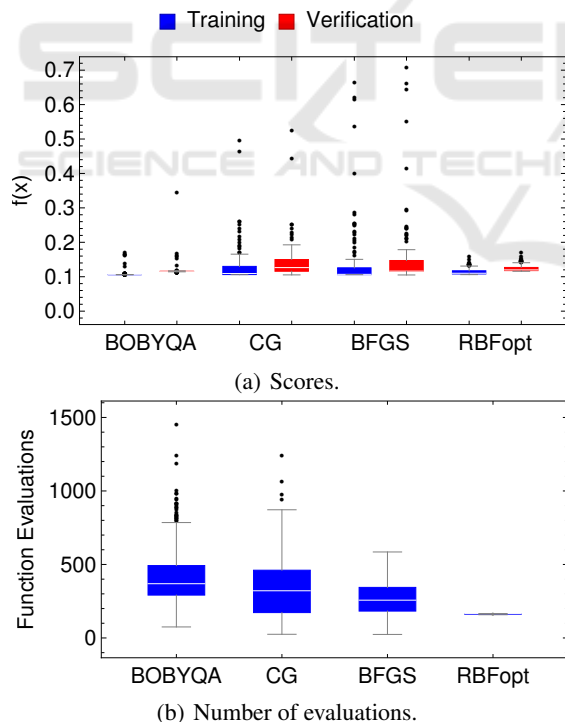


Figure 1: Boxplots showing final scores on the training and verification data sets and number of function evaluations of each algorithm on the robot controller simulation optimization problem.

5 GLOBAL WORKCELL LAYOUT OPTIMIZATION

This section describes the actual workcell optimization. To illustrate the method two scenarios are first described and the challenge in optimizing the objective is analysed. Secondly the section presents the proposed method of using Gaussian penalties for escaping local minima, followed by a strategy for sampling of starting points utilizing knowledge of the workcell. At the end the section introduces alternative optimization algorithms used for comparison in the experiment section.

5.1 Scenarios

Two scenarios are used for the workcell optimization. Both scenarios include picking randomly placed objects based on camera information and placing them for further operations.

5.1.1 Scenario 1: Bin Picking

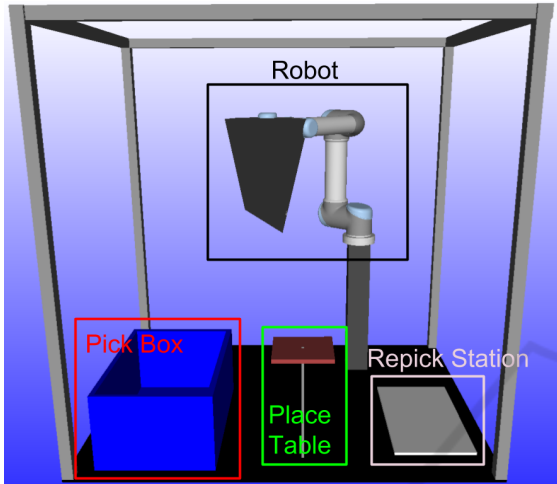
The bin picking scenario (BP), Figure 2(a), contains a 6 degree of freedom (DOF) Universal Robots UR5, a bin with randomly placed objects, a re-picking station and a place table. The robot picks objects from the bin and places them on the re-picking station for a more precise grip, before placing on the table. The reachability for this scenario is calculated from objects randomly placed in the bin and the execution times consists of moving the robot from the grasp position via the re-picking station and to the place table. To reduce redundancy in the optimization the robot is fixed in the workcell, but the three other components can be translated in XYZ and rotated around Z, giving a total of 12 parameters to optimize. The lower and upper bounds is set to assure that no part of the components are placed outside the frame comprising the workcell. Reachability in this scene is weighted ten times higher than execution times in the objective function.

5.1.2 Scenario 2: Industrial Assembly

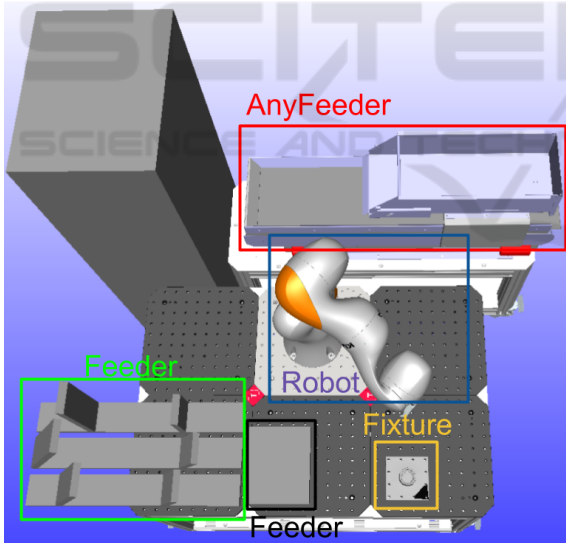
The industrial assembly scenario (IA), Figure 2(b), consists of a Kuka LBR IIWA 7 robot with 7 DOF and an attached Weiss WGS25 gripper, an Adept AnyFeeder with randomly placed objects on its feed surface, two feeders with fixed object positions and a fixture for assembling all the parts. Three different objects are picked from the AnyFeeder and one object from each of the two feeders with fixed objects. The objects are assembled in the fixture by simply placing

Table 1: Results of the robot controller simulator optimization after 250 runs, shown as mean scores on the training- and verification set and function evaluations along with their 99% confidence intervals.

	Training Scores	Verification Scores	Fnc. Evaluations
BOBYQA	0.106±0.00055	0.116±0.00110	407.1±19.4
CGD	0.127±0.00944	0.140±0.00943	340.7±22
BFGS	0.174±0.04630	0.186±0.04658	255.6±12.5
RBFopt	0.113±0.00120	0.123±0.00120	164.4±0.2



(a) Bin picking scenario



(b) Industrial assembly scenario.

Figure 2: The two scenes used for workcell layout optimization. Figure 2(a) shows the Bin Picking scenario and Figure 2(b) shows the industrial assembly scenario.

them on top of each other. The AnyFeeder is fixed in this scenario, meaning that the robot, the fixture and the two feeders can be translated in XYZ and rotated around the Z axis, giving a total of 16 parameters to optimize. The bounds make sure that none of the components can leave the platform on which they

are located, but they can be raised above it to a certain height. The reachability is weighted 100 times more than the execution time in this scene, as execution times are longer than in the BP scenario due to the higher number of motions. As the robot is a 7 DOF robot, there might potentially exist infinitely many inverse kinematics solutions to each of the transformations the TCP has to reach. One solution is to use a Jacobian based inverse kinematics solver (see e.g. (Buss, 2004)), finding only a single solution which may risk being in collision or violate joint limits. Instead an inverse kinematics solver is used, where the fourth joint is given an arbitrary configuration after which a closed form solver gives up to 8 possible inverse kinematics solutions. For the first pick position these are sorted favoring solutions where all joints are close to the middle of their limits, while for the next positions, solutions are sorted based on their distance in joint space to the previous chosen solution.

5.2 Gaussian Penalty Optimization

Slices of the objective function can be visualized as in Figure 3, where a discrete heat map is used to illustrate the objective function as the XY position of the pick area in the BP scenario is changed. From these views it becomes evident that the objective suffers from local minima, especially in the region connecting the blue to the red areas. These local minima will create problems for local optimization methods. Since the local minima appears to be shallow, the proposed method attempts to locally modify the objective and is based on the Fill Algorithm (Morris, 1993), presented in Algorithm 1.

Algorithm 1: Fill Algorithm.

```

while current state IS NOT solution do
  if current state IS NOT local minimum then
    └ make local change reducing cost
  else
    └ increase cost of current state
    
```

The Fill Algorithm is only proven complete in discrete cases, but we will argue that as the resolution

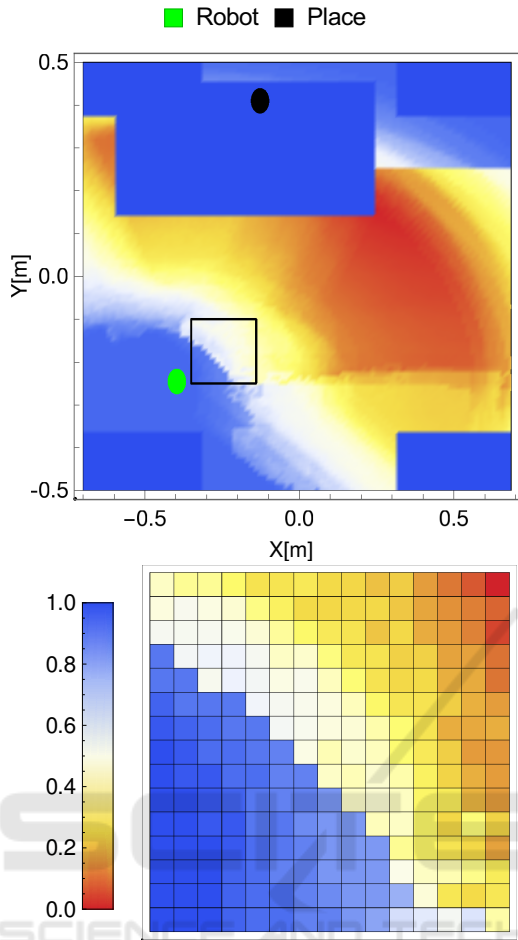


Figure 3: A slice of the discretized objective function when fixing all parameters of the BP scenario except XY translation of the pick box, along with an example close up of the marked square.

goes towards infinity, the found solution will go towards the solution in the continuous case. In the continuous case we cannot just increase the cost of a single state, but will rather locally modify the objective using a Gaussian kernel. This idea is illustrated in Algorithm 2.

Algorithm 2: GPopt - Gaussian Penalty Optimization.

Input:

Starting guess x , Objective function $f(x)$

$\hat{f}(x) \leftarrow f(x)$

$\hat{x} \leftarrow x$

while NOT DONE do

$\tilde{x} \leftarrow \text{OptimizeLocal}(\hat{x}, \hat{f}(x))$
 $\hat{f}(x) \leftarrow \hat{f}(x) + \mathcal{N}(\tilde{x}, |\tilde{x} - \hat{x}| \cdot \tau)$
 $\hat{x} \leftarrow \tilde{x}$

Informally the algorithm, which is referred to as Gaussian Penalty Optimization (GPopt), searches for a local minimum from the current starting point using a local optimization algorithm and penalizes that minimum in the objective function with a Gaussian normal distribution. The standard deviation is chosen based on the distance between the local minimum and the starting point, multiplied by a constant, τ , depending on the range of the objective function.

The stopping criterion of the algorithm can be chosen as either a maximum of time, iterations or improvement ratio. In this paper the local optimization is done with BOBYQA while the stopping criterion is based on the improvement ratio.

5.3 Improved Sampling Utilizing Robot Workspace Knowledge

Unlike general global optimization methods, GPopt relies on finding a feasible starting point from which it will search for a solution. The quality of the chosen starting point is therefore important for how quickly the algorithm finds the solution. The simplest strategy is to randomly sample until a feasible starting point is found, but by integrating some knowledge of the workcell into the sampling, better starting points can be found.

To that end, a sampling strategy exploiting the robots reach is implemented. Components are sampled in a band on a sphere around the robots base. One way of doing so, is to randomly sample spherical coordinates θ and ϕ , but this approach is biased towards the poles. Instead the method proposed by (Marsaglia et al., 1972) is used, where random points x_1 and x_2 are sampled from uniform distributions $(-1, 1)$ and rejected if $x_1^2 + x_2^2 \geq 1$, for the not-rejected points

$$x = 2x_1 \sqrt{1 - x_1^2 - x_2^2} \quad (6)$$

$$y = 2x_2 \sqrt{1 - x_1^2 - x_2^2} \quad (7)$$

$$z = 1 - 2(x_1^2 + x_2^2) \quad (8)$$

have a uniform distribution on the unit sphere and can be scaled to a desired radius. As only a band around the robot is wanted and not a full sphere, coordinates are translated to spherical coordinates and rejected depending on limits of θ .

This method do neglect parts of the sampling space, but it seems a fair assumption that feasible starting points lie within a sphere surrounding the robot, and since an arbitrary number of starting points can be sampled, the method is asymptotically complete in the space covered by this sphere.

In the IA scenario, where the AnyFeeder is fixed, the robots base coordinates are first sampled in a sphere around the AnyFeeder, and afterwards components in the scene are sampled around the robot.

5.4 Algorithms

The algorithms tested against GPopt, is described underneath. Only global derivative-free algorithms are chosen, assuming there exists a lot of local minima in the objective function and the derivative only can be found numerically. To cover the spectrum of different types of optimization algorithms, one deterministic, one model-based and one stochastic algorithm is chosen.

5.4.1 DIRECT

The DIRECT (DIviding hyperRECTangle) algorithm (Jones et al., 1993) is chosen to represent the deterministic category. DIRECT is a development of the classic Lipschitzian based methods, where a known Lipschitz constant is used to partition the search space until a solution is found. The two drawbacks of these methods are that the Lipschitz constant is unknown and that function evaluations increases exponentially with the parameter space. DIRECT fixes these problems by terminating once a predefined limit of iterations is reached and evaluating function values in the center of partitions instead of the extreme points. The implementation of the DIRECT algorithm is from the DAKOTA library, see (Adams et al., 2016).

5.4.2 RBFopt

RBFopt (Radial Basis Function optimization), (Gutmann, 2001), is the chosen model-based approach. It relies on Radial Basis Functions as surrogate models for approximating the objective function and guiding the search in the right direction. The model is refined to balance exploitation and exploration on global scale, and the used implementation is from (Costa and Nannicini, 2014).

5.4.3 EA

The EA (Evolutionary Algorithm) is chosen as the stochastic optimization algorithm. It was first introduced in (Holland, 1975) and relies on an approach resembling that of natural selection and reproduction guided by rules dictating survival of the fittest. Individuals are associated with a fitness score (objective function value) that probabilistically determines their chance of survival and reproduction. The used implementation is also from the DAKOTA library.

6 EXPERIMENTAL RESULTS

This section presents the experimental results of the paper. In Section 6.1 a small experiment determining the number of sample points to use is described. This is then followed by the actual workcell optimization in Section 6.2, which includes both some quantitative results comparing the different optimization algorithm and qualitative results of the workcell layouts.

6.1 Test of Number of Objects to Simulate

To determine how the number of samples used in the objective function influences the quality a set of experiments has been performed where a random workcell layout is generated and the objective function is calculated for 1 and up to 150 samples. In Figure 4 results are presented, where the objective function evaluations can be seen.

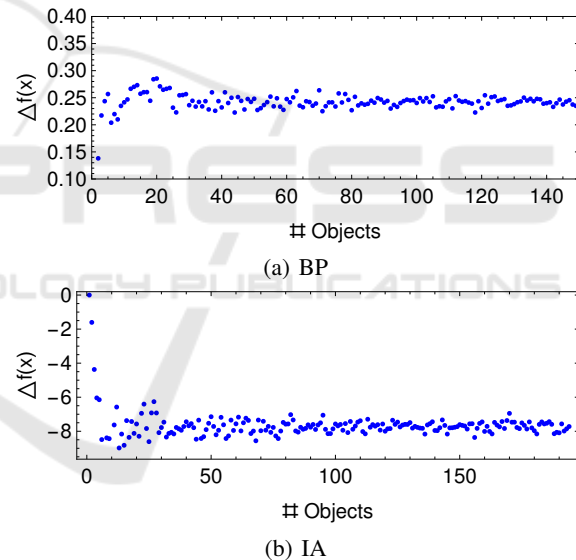


Figure 4: Evaluations the objective function on different number of simulated objects.

The differences in evaluations never reach 0 in any of the two scenarios, but manages to settle down on a more stable level when 30 objects are used in the BP scenario and 40 in the IA. These numbers of objects are therefore used in the optimization.

6.2 Test of Algorithms on Workcell Layout

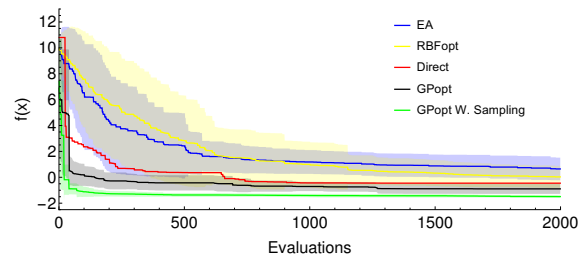
Figure 5 shows how the different optimization algorithms improves the objective as a function of the number of evaluations.

Evaluating the objective score per simulated object takes approximately 0.85 and 1.25 seconds for the two scenarios respectively. Given that 30 and 40 objects are simulated in each of the scenarios per function evaluation, is the computational burden of the optimization algorithms themselves considered negligible. Hence, only the number of evaluated scenarios are examined in the results.

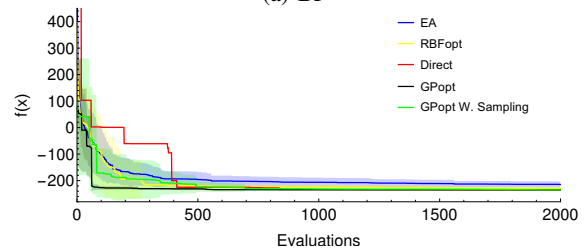
Since the RBFopt, EA and GPopt algorithms all depends on a sampling they have been run 50 times to reliably compute the means and standard deviations illustrated in the figure. For the GPopt algorithm a standard version using random samples as well as a variation, GPopt W. Sampling, using the improved sampling technique of Section 5.3 are included. The DIRECT method is deterministic, hence has no variance associated. In Table 2 the algorithms are compared based on their final best score for each run and the number of valid evaluations, meaning number of objective function evaluations where the workcell layout did not result in collisions or lacking inverse kinematics solutions for required target positions.

All in all the EA and RBFopt performs the worst in the two scenarios looking at both the function scores and the number of valid evaluations, where EA in average only evaluates 0.56% valid workcell layouts on the BP scenario, and RBFopt only 6.47%. These numbers are presumably also the reason for their low objective function scores, as the invalid workcell layouts gives little or no information of where to look for good workcell layouts in the parameter space. The DIRECT algorithm has more valid evaluations than the two aforementioned algorithms, but not as many as the two proposed methods. Even so, it manages to find an equally good solution in the IA scenario while a bit worse on the BP scenario.

GPopt with and without spherical sampling finds the best solutions. For the BP scenario, utilizing workspace knowledge for sampling is a bigger advantage than in the IA scenario, where results with and without are similar. Noteworthy for both scenarios, is that GPopt W. Sampling evaluates more invalid workcell layouts than without, but still reaches equal or better scores, indicating that the sampler manages



(a) BP



(b) IA

Figure 5: Workcell optimization results for the two scenarios, results are shown as the mean along with 2 standard deviations of the mean. The results are generated based on 50 optimizations for each of the algorithms.

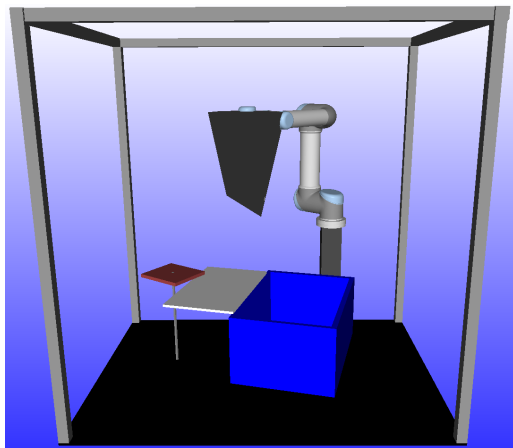
to find more optimal layouts that lies in between invalid layouts in the parameter space.

In Figure 7 a single run on the BP scenario for each of the algorithms are shown. Each orange dot corresponds to the score of a single evaluation and the blue line shows the minimum. Corresponding well with results in Table 2, EA and RBFopt evaluates a lot of invalid parameter sets. EAs evaluations seems to be coming rather sporadically whereas RBFopt manages to evaluate chunks of valid parameters sets. DIRECT finds more and more valid parameter sets as it moves along, due to its exploitation strategy. For the GPopt with and without spherical sampling, 5 and 6 start points are investigated respectively, where each starting leads to a lot of local minima. For the GPopt one optimization from starting point to the found minima is marked inside two dashed lines. Notable is that the spherical sampling has better starting points, therefore also reaches a better result in the end.

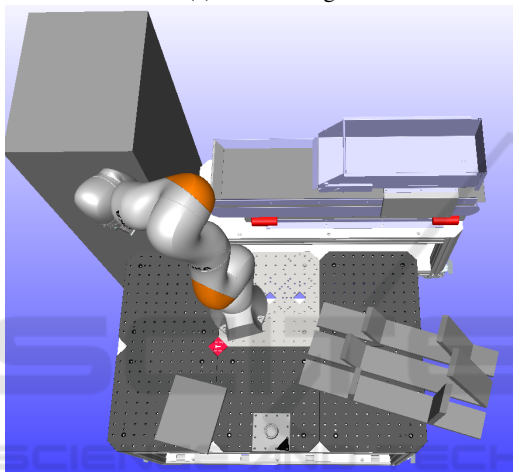
The workcell layouts that get the highest scores

Table 2: Results of workcell optimization on the two scenes. Results are shown as mean along with \pm two standard deviations for the evaluation scores.

	BP		IA	
	Valid Evaluations	Scores	Valid Evaluations	Score
EA	0.56%	0.64463 \pm 0.871404	2.07%	-218.457 \pm 7.94465
RBFopt	6.47%	-0.0495001 \pm 0.747906	18.43%	-229.132 \pm 4.35685
DIRECT	72.3%	-0.45452 \pm 0	50.91%	-234.435 \pm 0
GPopt	85.15%	-0.894707 \pm 0.386961	88.45%	-234.939 \pm 1.68963
GPopt W. Sampling	80.77%	-1.49056 \pm 0.0978638	87.22%	-234.944 \pm 4.90666



(a) Bin Picking



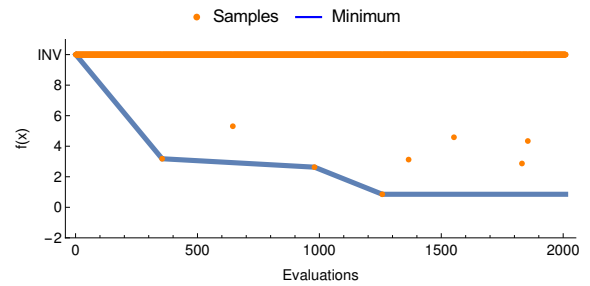
(b) Industrial Assembly

Figure 6: The best workcell layouts accomplished with the optimization algorithms, both come from GPopt with spherical sampling.

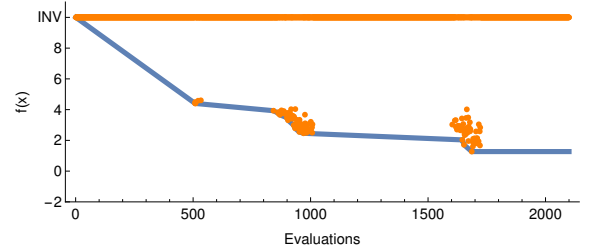
can be seen in Figure 6. Both layouts have components placed in a circle around the robot, in the band where reachability of the robot is highest and placed close together to lower the execution times as much as possible. In both scenarios are components rearranged compared to Figure 2 to accommodate for the order in which objects are moved. Furthermore is the robot placed higher than the other components in both scenarios, presumably to gain even more reachability.

7 CONCLUSION

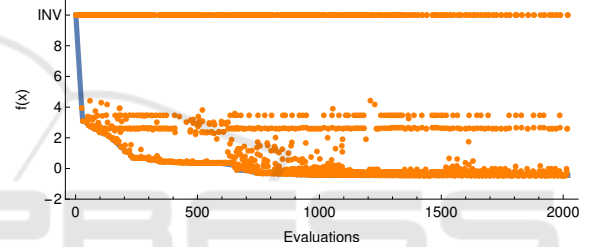
This paper has presented the problem of optimizing workcell layouts for two different industrial workcell setups, and suggested an optimization method for solving such problems, where a lot of local minima exist. The objective function is dependent on the



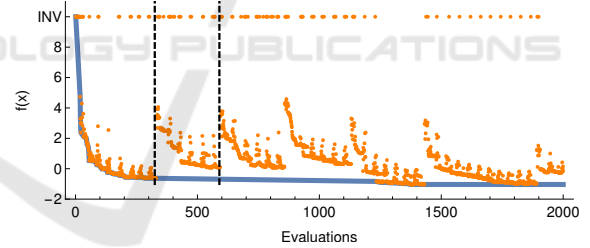
(a) EA



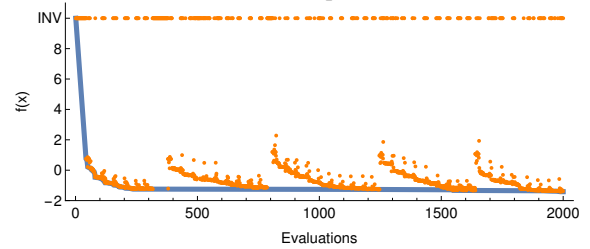
(b) RBFopt



(c) DIRECT



(d) GPopt



(e) GPopt with spherical sampling

Figure 7: Evaluations of the 5 algorithms on the BP scenario. Invalid parameter evaluations are defined as *INV* in the plots.

robots reachability and time spent on moving objects in the workcell estimated by an optimized simulation of the robot controller. Based on the Fill Algorithm,

which is proven to find an optimum if one exists, this paper suggests an optimization algorithm that iteratively optimizes towards local minima and tries to escape by penalizing the state by adding a Gaussian kernel to the objective function. As the algorithm depends on a starting point, a sampling method is suggested that samples workcell components in a sphere around the robot to maximize reachability of the robot. The algorithm is tested against other global optimization methods and a performance increase is demonstrated on the two scenarios.

REFERENCES

- ABB Robotics (2017). Robotstudio. <http://new.abb.com/products/robotics/robotstudio>. [Online; accessed 10-May-2017].
- Adams, B. M., Coleman, K., Hooper, R. W., Khuwaileh, B. A., Lewis, A., Smith, R. C., Swiler, L. P., Turinsky, P. J., and Williams, B. J. (2016). User Guidelines and Best Practices for CASL VUQ Analysis Using Dakota. Technical report, Sandia National Laboratories (SNL-NM), Albuquerque, NM (United States).
- Arabani, A. B. and Farahani, R. Z. (2012). Facility location dynamics: An overview of classifications and applications. *Computers & Industrial Engineering*, 62(1):408–420.
- Barraquand, J., Langlois, B., and Latombe, J.-C. (1992). Numerical potential field techniques for robot path planning. *IEEE Transactions on Systems, Man, and Cybernetics*, 22(2):224–241.
- Barraquand, J. and Latombe, J.-C. (1991). Robot motion planning: A distributed representation approach. *The International Journal of Robotics Research*, 10(6):628–649.
- Bélisle, C. J., Romeijn, H. E., and Smith, R. L. (1993). Hit-and-run algorithms for generating multivariate distributions. *Mathematics of Operations Research*, 18(2):255–266.
- Buss, S. R. (2004). Introduction to inverse kinematics with jacobian transpose, pseudoinverse and damped least squares methods. *IEEE Journal of Robotics and Automation*, 17(1-19):16.
- Cagan, J., Degentesh, D., and Yin, S. (1998). A simulated annealing-based algorithm using hierarchical models for general three-dimensional component layout. *Computer-aided design*, 30(10):781–790.
- Costa, A. and Nannicini, G. (2014). RBFOpt: an open-source library for black-box optimization with costly function evaluations. *Optimization Online*, (4538).
- FANUC (2017). ROBOGUIDE - FANUC Simulation Software. <http://robot.fanucamerica.com/products/vision-software/roboguide-simulation-software.aspx>. [Online; accessed 10-May-2017].
- Gonçalves, J. F. and Resende, M. G. (2015). A biased random-key genetic algorithm for the unequal area facility layout problem. *European Journal of Operational Research*, 246(1):86–107.
- Guan, J. and Lin, G. (2016). Hybridizing variable neighborhood search with ant colony optimization for solving the single row facility layout problem. *European Journal of Operational Research*, 248(3):899–909.
- Gueta, L. B., Chiba, R., Arai, T., Ueyama, T., and Ota, J. (2009). Compact design of work cell with robot arm and positioning table under a task completion time constraint. In *Intelligent Robots and Systems, 2009. IROS 2009. IEEE/RSJ International Conference on*, pages 807–813. IEEE.
- Gutmann, H.-M. (2001). A radial basis function method for global optimization. *Journal of global optimization*, 19(3):201–227.
- Holland, J. H. (1975). Adaptation in natural and artificial systems. an introductory analysis with application to biology, control, and artificial intelligence. *Ann Arbor, MI: University of Michigan Press*.
- Iversen, T. F. and Ellekilde, L.-P. (2017). Benchmarking motion planning algorithms for bin-picking applications. *Industrial Robot: An International Journal*, 44(2):189–197.
- Jones, D. R., Perttunen, C. D., and Stuckman, B. E. (1993). Lipschitzian optimization without the lipschitz constant. *Journal of Optimization Theory and Applications*, 79(1):157–181.
- King, D. E. (2009). Dlib-ml: A machine learning toolkit. *Journal of Machine Learning Research*, 10(Jul):1755–1758.
- Kirkpatrick, S., Gelatt, C. D., Vecchi, M. P., et al. (1983). Optimization by simulated annealing. *Science*, 220(4598):671–680.
- Koopmans, T. C. and Beckmann, M. (1957). Assignment problems and the location of economic activities. *Econometrica: journal of the Econometric Society*, 25(1):53–76.
- LaValle, S. M. (1998). Rapidly-exploring random trees a new tool for path planning. Tech. rep., Iowa State Univ., Comp Sci. Dept.
- Lim, Z. Y., Ponnambalam, S., and Izui, K. (2016). Nature inspired algorithms to optimize robot workcell layouts. *Applied Soft Computing*, 49:570–589.
- Marsaglia, G. et al. (1972). Choosing a point from the surface of a sphere. *The Annals of Mathematical Statistics*, 43(2):645–646.
- Morris, P. (1993). The breakout method for escaping from local minima. In *Proceedings of the Eleventh National Conference on Artificial Intelligence*, volume 93, pages 40–45.
- Park, M. G. and Lee, M. C. (2003). A new technique to escape local minimum in artificial potential field based path planning. *KSME international journal*, 17(12):1876–1885.
- Petersen, H. G. and Ellekilde, L.-P. (2011). Modeling motions of a KUKA KR30 robot. Technical report, The Maersk Mc-Kinney Moller Institute, University of Southern Denmark.
- Powell, M. J. (2009). The BOBYQA algorithm for bound constrained optimization without derivatives. Techni-

cal report, Department of Applied Mathematics and Theoretical Physics, University of Cambridge.

- Rios, L. M. and Sahinidis, N. V. (2013). Derivative-free optimization: a review of algorithms and comparison of software implementations. *Journal of Global Optimization*, 56(3):1247–1293.
- Schulman, J., Duan, Y., Ho, J., Lee, A., Awwal, I., Bradlow, H., Pan, J., Patil, S., Goldberg, K., and Abbeel, P. (2014). Motion planning with sequential convex optimization and convex collision checking. *The International Journal of Robotics Research*, 33(9):1251–1270.
- Universal Robots (2017). Universal robots simulator software. <https://www.universal-robots.com/download>. [Online; accessed 10-May-2017].
- Yoshikawa, T. (1985). Manipulability of robotic mechanisms. *The international journal of Robotics Research*, 4(2):3–9.
- Zhang, J. and Li, A.-P. (2009). Genetic algorithm for robot workcell layout problem. In *Software Engineering, 2009. WCSE'09. WRI World Congress on*, volume 4, pages 460–464. IEEE.

